

Investigation of the Thermal, Structural and Optical Properties of $\text{Ni}_{0.8}\text{Mg}_{0.2}\text{Al}_{0.05}\text{Fe}_{1.95}\text{O}_4$ Nanoparticles Prepared by Sol-gel Combustion Method

Wondimagegn Anjulo Sisay

Department of Physics, College of Natural Sciences, Arba Minch University, Arba Minch, Ethiopia

Abstract—Nanocrystalline magnetic spinel $\text{Ni}_{0.8}\text{Mg}_{0.2}\text{Al}_{0.05}\text{Fe}_{1.95}\text{O}_4$ material was synthesized by sol-gel combustion method using nitrates and citric acid. The phase formation, structure as well as optical properties of the synthesized material were investigated using powder x-ray diffraction (XRD), Fourier transform infrared (FTIR) spectroscopy and ultraviolet-visible (UV-vis) spectroscopy. Different structural parameters including lattice constant, unit cell volume, crystal size, Debye temperature and optical band gap of $\text{Ni}_{0.8}\text{Mg}_{0.2}\text{Al}_{0.05}\text{Fe}_{1.95}\text{O}_4$ sample were also estimated. The XRD result revealed that the synthesized $\text{Ni}_{0.8}\text{Mg}_{0.2}\text{Al}_{0.05}\text{Fe}_{1.95}\text{O}_4$ sample possessed a single-phase cubic spinel structure with Fd-3m space group without the presence of other phase impurities. The lattice parameter and the average crystal size of $\text{Ni}_{0.8}\text{Mg}_{0.2}\text{Al}_{0.05}\text{Fe}_{1.95}\text{O}_4$ sample were also found to be 8.3406 Å and 52 nm, respectively. This confirmed the nanocrystalline nature of the synthesized material. The FT-IR analysis of the synthesized material revealed the presence of two strong absorption bands of the tetrahedral and octahedral groups in the expected range of cubic spinel-type ferrites. The combined results of XRD and FTIR confirmed that the substitution of Mg^{3+} for Ni^{2+} and Al^{3+} for Fe^{3+} did not change the basic structure of the spinel NiFe_2O_4 ferrite particles. Further, the optical bandgap energy of $\text{Ni}_{0.8}\text{Mg}_{0.2}\text{Al}_{0.05}\text{Fe}_{1.95}\text{O}_4$ nanoparticles calculated experimentally was found to be 3.48 eV, indicating the semiconductor behavior of $\text{Ni}_{0.8}\text{Mg}_{0.2}\text{Al}_{0.05}\text{Fe}_{1.95}\text{O}_4$ sample.

Keywords: Nanocrystalline, Sol-gel combustion, Structure, Optical property.

1. INTRODUCTION

Nanomaterials play a pivotal role in physical, chemical and biomedical fields due to their high surface energies. Advanced functional materials for various technological applications are under extensive study. Among various types of advanced materials, the ferrites are important magnetic materials due to their versatile use in electromagnetic applications. Synthesis and application of nanomaterials is the subject of intense research because of their unique physical and chemical properties, which makes them very appealing in view of both, the scientific value of understanding their properties and the technological significance of enhancing the performance of existing

materials [1]. There are two main factors which make nanomaterials to behave significantly different from that of bulk materials. The first one is the surface effects which cause the smooth properties scaling due to the fraction of atoms at the surface and the second one is the quantum effects which cause the discontinuous behavior due to quantum confinement effects in materials with delocalized electrons [2]. These factors affect the chemical reactivity of materials and physical properties such as the structure, mechanical, optical, electrical and magnetic properties.

The electrical, dielectric, magnetic, thermal and structural properties of the magnetic semiconductor ferrites are very sensitive to the chemical composition, type and amount of additives, sintering temperature and time [3]. It is well known that when ferrites are sufficiently diluted with non-magnetic atoms, they can show a wide spectrum of magnetic order ranging from ferrimagnetism, anti-ferromagnetism, local canted spin to semi-spin glass and spin glass [4]. The magnetic behavior of ferrites is originated from the three kinds of super-exchange interactions A-B, A-A and B-B which are mediated by the intermediate O^{2-} ions. The magnetic properties of ferrite are divided into intrinsic or structure-insensitive. Saturation magnetization and Curie temperature are the two prominent structure-insensitive properties. While, induction, permeability, hysteresis loop, coercive force and remnance belong to extrinsic or structure-sensitive.

Several methods such as solid state reaction, sol-gel, hydrothermal, combustion, co-precipitation are employed to synthesize ferrite nanoparticles. Solid state reaction method is economical for the bulk synthesis of ferrites but undesired non-uniform particles are formed due to aggregation and phase purity is not completely achieved. However, ferrite nanoparticles synthesized by sol-gel, hydrothermal, combustion, co-precipitation possess good chemical homogeneity and high purity. The sol-gel combustion method, in particular, is one of the most useful and attractive techniques for the synthesis of nanosized ferrite materials because of its advantages such as good stoichiometric control and the production of ultrafine particles with a narrow size distribution in a relatively short processing time at very low temperature. This method is originated from the combined sol-gel and combustion methods. Sol-gel synthesis

method refers to the hydrolysis and condensation of metal alkoxides or alkoxide precursors, leading to dispersions of oxide particles in a "sol". The "sol" is then dried or "gelled" by solvent removal or by chemical reaction. In sol-gel method, water is used as the solvent, but the precursors can also be hydrolyzed by an acidic or basic medium. The catalysis process induces the formation of colloidal as well as polymeric form of the gel [5,6]. Solution combustion technique is a technique with a unique combination of the chemical and the combustion processes. In combustion synthesis method, organic acids like formic acid, citric acid or glycolic acid is used as a fuel and cations chelating agent.

Basically, ferrites are three types: spinel, garnet and magneto-plumbite. Iron based spinel ferrites are compounds having a general formula of AFe_2O_4 , in which the A represents the divalent cations such as Ni^{2+} , Zn^{2+} , Cu^{2+} , Co^{2+} etc. These types of ferrites are useful magnetic materials because of their low cost and high electromagnetic performance over a wide frequency range as compared to the pure metals [7]. They are also widely used in electronic and magnetic devices due to their high magnetic permeability and low magnetic losses [8]. In the recent years, iron based spinel ferrite nanoparticles have received great attention due to their applications in the diverse fields like medical applications such as for magnetic resonance imaging [9] and cancer therapy [10]. They are also used for mineral separation, magnetic storage devices [11], catalysis [12], magnetic refrigeration system, drug delivery system [13], and sensors.

Nickel ferrite is a soft ferrimagnetic material with spinel structure having a general chemical formula of $NiFe_2O_4$ with face centered cubic lattice structure. $NiFe_2O_4$ ferrite has an inverse spinel structure with all Ni^{2+} ions located in the octahedral sites and Fe^{3+} ions occupying tetrahedral and octahedral sites. $NiFe_2O_4$ ferrite can exhibit interesting electrical, dielectric and magnetic properties in the monocrystalline form compared to those of bulk form. The mixed spinel Ni-Mg magnetic materials have very wide technological applications. Currently, intensive research work is conducted on these materials. Different researchers reported the effect of substitution of Zn, Mg, Co, Cd, Cu, etc. cations on structural, electrical and magnetic properties of Ni-Mg ferrite materials. A literature survey shows that the thermal, structural, optical, electrical and magnetic behavior of Ni-Mg nanoparticles depends mainly on the particles size and the type of synthesis method utilized. Recently, different methods have been employed to synthesize highly crystalline and uniformly sized magnetic nanoparticles of Ni-Mg based compound. In this study, $Ni_{0.8}Mg_{0.2}Al_{0.05}Fe_{1.95}O_4$ nanoparticles was synthesized by so-gel combustion method using nitrates as the raw materials and citric acid as a fuel and chelating agent. The phase formation, structure and optical property of this compound were investigated by using different advanced characterization techniques.

2. MATERIALS AND METHODS

2.1. Synthesis Procedures

Nanocrystalline $Ni_{0.8}Mg_{0.2}Al_{0.05}Fe_{1.95}O_4$ sample was synthesized by sol-gel combustion method. $Ni(NO_3)_2 \cdot 6H_2O$, $Mg(NO_3)_2 \cdot 6H_2O$, $Al(NO_3)_3 \cdot 9H_2O$, $Fe(NO_3)_3 \cdot 9H_2O$ and citric acid monohydrate ($C_6H_8O_7 \cdot H_2O$) were used as raw materials for the synthesis process. Initially, the stoichiometric amounts of $Ni(NO_3)_2 \cdot 6H_2O$, $Mg(NO_3)_2 \cdot 6H_2O$, $Al(NO_3)_3 \cdot 9H_2O$ and $Fe(NO_3)_3 \cdot 9H_2O$ precursors was dissolved in double distilled water and stirred for about 15 minutes. The stoichiometric amount of citric acid was dissolved in distilled water in separate beaker and stirred for about 10 minutes. Further, this citric acid solution was then added in to the solution of nitrates. The ratio of metal nitrates to citric acid was 1:1. The solution was further stirred for about 20 minutes with magnetic stirrer and ammonia solution was then added under constant stirring in order to make the pH value 7. The resulting solution was continuously heated on the magnetic stirrer at $50^\circ C$ to form a gel. When the obtained gel is further heated at $90^\circ C$, combustion process was conducted in the hottest zones of the beaker and propagated to self-ignition from the bottom to the top like the eruption of a volcano. Further, the obtained black powder was ground in an agate mortar for about 2 hours and heated at $950^\circ C$ for 8 hours in air furnace. Finally, this powder was ground for an hour using an agate mortar and pestle. The detail of the synthesis procedure is shown in Fig. 1.

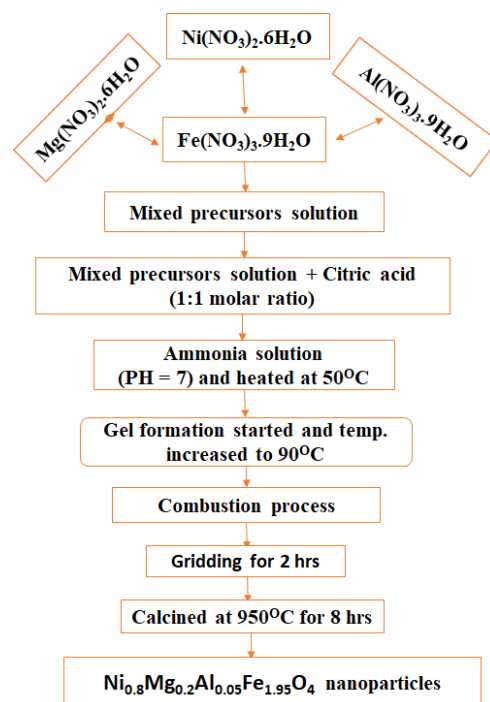


Figure-1: Flow chart of the sol-gel combustion synthesis procedure.

2.2. Material Characterizations

Powder X-ray diffraction pattern was recorded using X-ray diffractometer (XRD-7000S diffractometer) with a Cu K α radiation of wavelength $\lambda = 1.5406 \text{ \AA}$ source. The measurement was conducted between a diffraction angle of $2\theta = 10^\circ$ and 80° . FT-IR spectroscopy measurement was accomplished by IR AFFINITY-1S shimadzu instrument in transmittance method with potassium Bromide (KBr) as IR window in the wavenumber region of 350 to 4000 cm^{-1} . The optical energy band gap of $\text{Ni}_{0.8}\text{Mg}_{0.2}\text{Al}_{0.05}\text{Fe}_{1.95}\text{O}_4$ nanoparticles was investigated by using Uv-vis spectroscopy (Specord 50 plus instrument) in the wavelength range from 200 to 800 nm .

3. RESULTS AND DISCUSSION

3.1. XRD analysis

The crystal structure and the phase formation of the synthesized $\text{Ni}_{0.8}\text{Mg}_{0.2}\text{Al}_{0.05}\text{Fe}_{1.95}\text{O}_4$ material was identified by using X-ray diffraction technique in the range of 2θ between 20° and 80° after the sample is calcined at 950°C for 8 hours. The obtained room temperature XRD pattern of $\text{Ni}_{0.8}\text{Mg}_{0.2}\text{Al}_{0.05}\text{Fe}_{1.95}\text{O}_4$ powder sample synthesized by sol-gel combustion method is shown in Fig. 2. All the peaks appeared in the XRD pattern are well-defined and very sharp, suggesting the high crystallinity of the synthesized material. The XRD pattern is also confirmed the pure phase formation of $\text{Ni}_{0.8}\text{Mg}_{0.2}\text{Al}_{0.05}\text{Fe}_{1.95}\text{O}_4$ powder sample without any impurity. The crystalline phase of the synthesized sample is identified as a single phase cubic spinel structure with Fd-3m space group of NiFe_2O_4 spinel. The diffraction peaks obtained at 2θ values of $30.07, 35.40, 36.85, 43.00, 53.33, 56.86, 62.44, 65.19$ and 74.14° correspond to (111), (220), (311), (222), (400), (422), (511), (440), (620) and (533) planes, respectively which can be readily correspond to the formation of a single phase cubic spinel structure of $\text{Ni}_{0.8}\text{Mg}_{0.2}\text{Al}_{0.05}\text{Fe}_{1.95}\text{O}_4$ material. The obtained these XRD peaks are also indexed using the Joint Committee on Powder Diffraction Standards (JCPDS) card with good agreement for NiFe_2O_4 (card no. 86-2267).

The lattice parameter (a) and the unite cell volume (V) of $\text{Ni}_{0.8}\text{Mg}_{0.2}\text{Al}_{0.05}\text{Fe}_{1.95}\text{O}_4$ material were evaluated from (400) plane using the relations [14];

$$a = d\sqrt{h^2 + k^2 + l^2} \text{ and}$$

$$V = a^3$$

where 'd' is the inter-planar spacing, 'h,k, and l' are Miller indices. Moreover, the average crystallite size (L) of $\text{Ni}_{0.8}\text{Mg}_{0.2}\text{Al}_{0.05}\text{Fe}_{1.95}\text{O}_4$ material was calculated from (311) plane using Scherrer's formula [14];

$$L = \frac{0.9 \lambda}{\beta \cos \theta}$$

where ' λ ' is the wavelength of Cu K α source ($\lambda = 1.5406 \text{ \AA}$), ' β ' is the full width at half maximum (FWHM) of the diffraction peak and ' θ ' is the diffraction angle. The obtained results are tabulated in Table 1. The lattice parameter and the unite cell volume of $\text{Ni}_{0.8}\text{Mg}_{0.2}\text{Al}_{0.05}\text{Fe}_{1.95}\text{O}_4$ material are found to be 8.3406 \AA and $580.2 (\text{ \AA})^3$, respectively. This shows that the obtained results are slightly lower than the reported values of the parent NiFe_2O_4 compound (8.3422 \AA and $580.6 (\text{ \AA})^3$) [15]. The variation in lattice constant as well as unite cell volume values can be explained on the basis of Vegard's law. According to this law, the variation in these structural parameters are related to the ionic radii of the substituted ions. In the present study, some amount of Ni^{2+} ion (ionic radius, 0.69 \AA) [16] is replaced by Mg^{2+} ion (ionic radius, 0.78 \AA) [16] and some amount of Fe^{3+} ion (ionic radius, 0.645 \AA) [17] is replaced by Al^{3+} (ionic radius, 0.535 \AA) [17]. Thus, the substitution of Ni^{2+} and Fe^{3+} ions with Mg^{2+} and Al^{3+} ions results in a slight decrease in lattice constant as well as unite cell volume of $\text{Ni}_{0.8}\text{Mg}_{0.2}\text{Al}_{0.05}\text{Fe}_{1.95}\text{O}_4$ material. Similar report has been made by Babu and Tatarchuk [17]. The average crystal size of $\text{Ni}_{0.8}\text{Mg}_{0.2}\text{Al}_{0.05}\text{Fe}_{1.95}\text{O}_4$ is also found to be 52 nm , which reveals the nanocrystalline nature of $\text{Ni}_{0.8}\text{Mg}_{0.2}\text{Al}_{0.05}\text{Fe}_{1.95}\text{O}_4$ material.

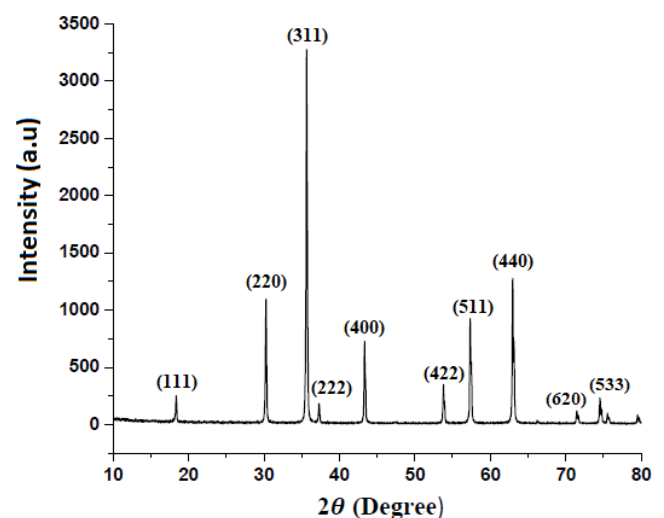


Figure-2: XRD pattern of $\text{Ni}_{0.8}\text{Mg}_{0.2}\text{Al}_{0.05}\text{Fe}_{1.95}\text{O}_4$ nanoparticles

The bond lengths between the metal and oxygen coordination at the tetrahedral (A) and octahedral (B) sites of spinel $\text{Ni}_{0.8}\text{Mg}_{0.2}\text{Al}_{0.05}\text{Fe}_{1.95}\text{O}_4$ nanoparticles were calculated using the relations [18,19];

$$A - O = a\sqrt{3} \left(u - \frac{1}{4} \right) \text{ and}$$

$$B - O = a \sqrt{3u^2 - \frac{11}{4}u + \frac{43}{64}}$$

Table - 1: Different structural parameters of the synthesized material.

Sample	2 θ value for (400) (degree)	d-spacing for (400) (Å)	FWHM for (311) (Degree)	Lattice Constant a (Å)	Unit Cell Volume V (Å) ³	Crystal Size L from (311) (nm)
Ni _{0.8} Mg _{0.2} Al _{0.05} Fe _{1.95} O ₄	43.3602	2.08514	0.16060	8.3406	580.2	52

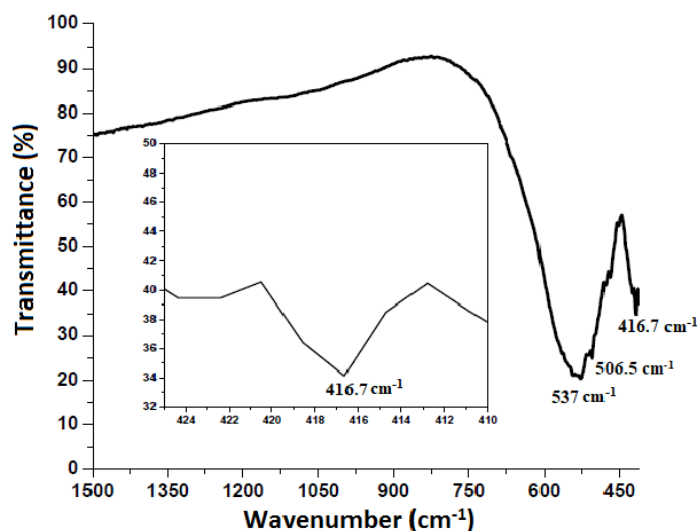
where 'u' is the oxygen positional parameter (0.381 Å) [20]. The bond lengths of both the tetrahedral and octahedral sites of spinel Ni_{0.8}Mg_{0.2}Al_{0.05}Fe_{1.95}O₄ nanoparticles are 1.9 and 2.05 Å, respectively. This indicates that the bond length of octahedral site is larger than the tetrahedral site in spinel Ni_{0.8}Mg_{0.2}Al_{0.05}Fe_{1.95}O₄ nanoparticles, which considers with the reported values of NiFe₂O₄ [19].

3.2. FT-IR analysis

The FTIR spectroscopy is a non-destructive characterization technique useful to investigate the structure of different types of ferrite materials. It gives an information about the chemical and molecular structure changes in the synthesized ferrite materials after calcination treatments. FTIR spectroscopy study can also give information about the position and occupation of the ions in the spinel lattice of ferrite materials. In ferrite materials, the metal cations are located at tetrahedral and octahedral sites according to the geometric configuration of the oxygen ions nearest neighbors. Different researchers reported that two main broad metal-oxygen absorption bands are present in the IR spectrum of spinel ferrite materials. The high frequency band ν_1 observed at around 600 cm⁻¹ represent the tetrahedral metal-oxygen vibration while the low-frequency band ν_2 observed at around 400 cm⁻¹ represent the octahedral metal-oxygen vibration in the spinel lattice of ferrite materials [19]. The variation in the position of the absorption bands formed in spinel ferrite materials is due to the difference in the bond strength between the metal-oxygen coordination in the octahedral and tetrahedral sites. Srivastava et al. [14] have investigated the FTIR spectrum of NiFe₂O₄ ferrite material. They reported that the absorption band ν_1 around 597.94 cm⁻¹ corresponds to the stretching vibrations of Fe³⁺-O band in tetrahedral sites and ν_2 around 397.21 cm⁻¹ is related to the stretching vibrations of Fe³⁺-O and Ni²⁺-O bands in tetrahedral sites.

The room temperature FTIR spectrum of Ni_{0.8}Mg_{0.2}Al_{0.05}Fe_{1.95}O₄ nanoparticles prepared by sol-gel combustion technique is shown in Fig. 3. It is seen that the FT-IR analysis of the synthesized material reveals the presence of two strong absorption bands ν_1 and ν_2 which lie in the expected range of cubic spinel-type ferrites [19]. The higher frequency band ν_1 which appears at 537 cm⁻¹ may be assigned to the stretching vibration of the metal-oxygen

bonding force of tetrahedral group in Ni_{0.8}Mg_{0.2}Al_{0.05}Fe_{1.95}O₄ lattice structure [21]. While, the lower frequency band ν_2 which appears at 416.7 cm⁻¹ may represent the metal-oxygen stretching vibration of octahedral group [21]. The presence of the two bands from the IR spectrum of Ni_{0.8}Mg_{0.2}Al_{0.05}Fe_{1.95}O₄ reveals the formation cubic spinel nanoferrite materials. Different researchers have identified that the normal mode of vibration of the tetrahedral cluster is higher than that of the octahedral cluster. This change is related to the shorter bond length of the tetrahedral cluster and the longer bond length of the octahedral cluster [16]. As it is seen in the figure, small band is observed around 506.5 cm⁻¹, which may be due to the stretching vibrations of Mg-O band. As compared with the bands of NiFe₂O₄ compound reported by Srivastava et al. [14], the absorption peak of in the octahedral Ni_{0.8}Mg_{0.2}Al_{0.05}Fe_{1.95}O₄ is shifted towards higher wavenumber region This predicts that Al³⁺ prefers octahedral sites. Moreover, the change in band position may be due to the substitution of Al³⁺ ions for Fe³⁺ ions leads to the decrease in metal-oxygen separation in the octahedral site. This is also in good agreement with the lower lattice parameter, unit cell volume and crystal size calculated from the XRD pattern.


Figure-3: FT-IR spectra of Ni_{0.8}Mg_{0.2}Al_{0.05}Fe_{1.95}O₄ nanoparticles.

The elastic force constants for tetrahedral site K_T and octahedral site K_o of Ni_{0.8}Mg_{0.2}Al_{0.05}Fe_{1.95}O₄ nanoparticles were calculated by using the relations;

$$K_t = 7.62 \times M_1 \times v_1^2 \times 10^{-7} \text{ N/m}$$

$$K_o = 10.62 \times \frac{M_2}{2} \times v_2^2 \times 10^{-7} \text{ N/m}$$

where M_1 is the molecular weight of cations at the tetrahedral site, M_2 is the molecular weight of cations at the octahedral site, v_1 is the frequency band at tetrahedral site and v_2 is also the frequency band at the octahedral site. The values of the elastic force constants for tetrahedral (K_t) and octahedral site (K_o) in $\text{Ni}_{0.8}\text{Mg}_{0.2}\text{Al}_{0.05}\text{Fe}_{1.95}\text{O}_4$ nanoparticles are found to be 1.23×10^5 dyne/cm and 9.7×10^4 dyne/cm. This confirms that the elastic force constant of K_t is larger than that of K_o , which is associated with the shorter bond length of tetrahedral cluster and longer bond length of octahedral cluster in $\text{Ni}_{0.8}\text{Mg}_{0.2}\text{Al}_{0.05}\text{Fe}_{1.95}\text{O}_4$ nanoparticles

The Debye temperature (D_T) (the temperature at which the maximum lattice vibrations take place) of $\text{Ni}_{0.8}\text{Mg}_{0.2}\text{Al}_{0.05}\text{Fe}_{1.95}\text{O}_4$ nanoparticles was evaluated using the relation [22];

$$D_T = \frac{hc v_{av}}{K} = 1.438 v_{av}$$

where $v_{av} = \frac{v_1 + v_2}{2}$ is the average value of the absorption bands, $\hbar = \frac{h}{2\pi}$, h is Planck's constant and C is the speed of light. The Debye temperature of $\text{Ni}_{0.8}\text{Mg}_{0.2}\text{Al}_{0.05}\text{Fe}_{1.95}\text{O}_4$ nanoparticles derived from FTIR data is found to be 685.7 K, which considers with the reported value of NiFe_2O_4 .

3.3. Optical property study

UV-vis spectral analysis has been widely used to characterize semiconductor nanoparticles. It is the easiest way to study the optical properties as well as estimating the optical band gap of a semiconductor materials. The optical band gap energy shows the energy that requires by an electron to excite from valence band to conduction band in the lattice of semiconductor materials. Several researchers reported that as the particle size of the semiconductor materials decreases, the absorption edge shifts to shorter wavelength, due to the band gap increase of the smaller particles. In this study, the UV-Visible spectroscopy study was conducted to investigate the optical properties of spinel $\text{Ni}_{0.8}\text{Mg}_{0.2}\text{Al}_{0.05}\text{Fe}_{1.95}\text{O}_4$ nanoparticles synthesized by sol-gel combustion method at a temperature of 950°C. This measurement was conducted in the wavelength range of 200 to 600 nm and the obtained spectrum is shown in Fig. 4. As it can be seen in the figure, spinel $\text{Ni}_{0.8}\text{Mg}_{0.2}\text{Al}_{0.05}\text{Fe}_{1.95}\text{O}_4$ nanoferrite has high absorbance in the wavelength region of 214 to 303 nm, which decreases gradually as the wavelength increases. The highest absorption spectrum is

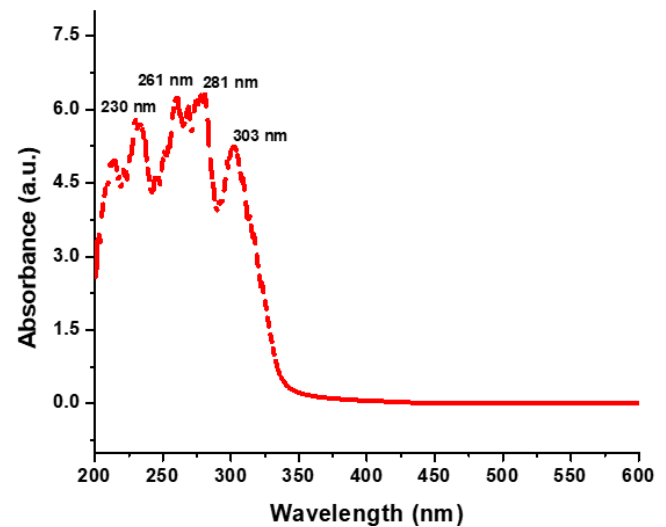


Figure-4: UV-vis spectrum of $\text{Ni}_{0.8}\text{Mg}_{0.2}\text{Al}_{0.05}\text{Fe}_{1.95}\text{O}_4$ nanoparticles

appeared at a wavelength of around 281 nm. From this it can be suggested that the prepared $\text{Ni}_{0.8}\text{Mg}_{0.2}\text{Al}_{0.05}\text{Fe}_{1.95}\text{O}_4$ nanoparticles are optically active, which is in accordance with the previously reported literature [23].

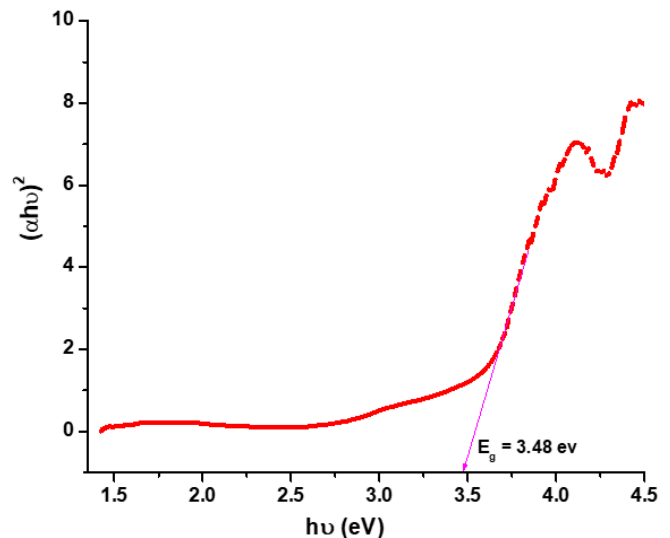


Figure-5: Energy band spectrum of $\text{Ni}_{0.8}\text{Mg}_{0.2}\text{Al}_{0.05}\text{Fe}_{1.95}\text{O}_4$ nanoparticles.

The optical band gap energy of $\text{Ni}_{0.8}\text{Mg}_{0.2}\text{Al}_{0.05}\text{Fe}_{1.95}\text{O}_4$ sample was calculated by using Tauc's relation [24];

$$\alpha hv = A(hv - E_g)^n$$

Where α is the absorption coefficient, hv is the photon energy, E_g is the band gap and the exponent n is used to determine the type of electronic transition and takes values of 1/2 for direct band gap, whereas for indirect band gap, n is equal to 2. The absorption coefficient ' α ' of the synthesized

material was determined from the absorption data by using the relation;

$$I = I_0 e^{-\alpha t}$$
$$A = \log(I/I_0)$$
$$\alpha = 2.303 (A/t)$$

where, I_0 is the intensity of the incident radiation, I is the intensity of the transmitted radiation and t is the thickness of the $\text{Ni}_{0.8}\text{Mg}_{0.2}\text{Al}_{0.05}\text{Fe}_{1.95}\text{O}_4$ ferrite sample. Further, to obtain the optical band gap of the sample, the graph of $(\alpha h\nu)^{1/2}$ versus $h\nu$ was plotted (Fig. 5). The intercept of the line at $\alpha = 0$ gives the value of energy band gap.

The value of the optical energy band gap for $\text{Ni}_{0.8}\text{Mg}_{0.2}\text{Al}_{0.05}\text{Fe}_{1.95}\text{O}_4$ nanoparticles synthesized by sol-gel combustion method is found to be 3.48 eV. This band gap energy of the synthesized sample is somewhat lower as compared to the band gap of $\text{Ni}_{0.3}\text{Cu}_{0.2}\text{Zn}_{0.5}\text{Fe}_2\text{O}_4$ ferrite (3.8 eV) [23]. This may be associated with the variation of the particle sizes of both compounds. Further, the obtained band gap result is also revealed that the synthesized sample has a semiconductor behavior.

3. CONCLUSIONS

Nanocrystalline spinel $\text{Ni}_{0.8}\text{Mg}_{0.2}\text{Al}_{0.05}\text{Fe}_{1.95}\text{O}_4$ magnetic material was successfully synthesized by sol-gel combustion method using *nickel nitrate, magnesium nitrate, aluminum nitrate and ferric nitrate precursors. Citric acid was also used as a fuel and chelating agent.* The XRD results revealed the formation of cubic spinel-type structure with lattice parameters and an average crystallite size of 8.3406 Å and 52 nm, respectively. The room temperature FTIR spectrum of $\text{Ni}_{0.8}\text{Mg}_{0.2}\text{Al}_{0.05}\text{Fe}_{1.95}\text{O}_4$ nanoparticles confirmed the formation of two strong absorption bands. The higher frequency band which appeared at 537 cm^{-1} assigned to the stretching vibration of the metal-oxygen bonding force of tetrahedral. The lower frequency band that appeared at 416.7 cm^{-1} represented the metal-oxygen stretching vibration of octahedral group. The combined results of XRD and FTIR confirmed that the substitution of Mg^{3+} for Ni^{2+} and Al^{3+} for Fe^{3+} did not change the basic structure the spinel NiFe_2O_4 ferrite particles. The calculated optical band gap energy was found to be 3.48 eV, indicating the semiconductor behavior of $\text{Ni}_{0.8}\text{Mg}_{0.2}\text{Al}_{0.05}\text{Fe}_{1.95}\text{O}_4$ nanoparticles.

ACKNOWLEDGEMENT

The author gratefully acknowledges Dr. Paulos Taddesse for his support. The author also acknowledges Dr. Vijaya Babu, Adama Science and Technology University and department of chemistry for conducting XRD, FTIR, UV-vis and VSM characterization.

REFERENCES

- [1] A. Ghasemi, A. M. Davarpanah, M. Ghadiri, Structure and Magnetic Properties of Oxide Nanoparticles of Fe-Co-Ni Synthesized by Co-Precipitation Method, International Journal of Nano science and Nanotechnology, vv. 8, 2012, pp. 207-214.
- [2] E. Roduner, Size matters: Why Nano materials are different, Chemical Society Reviews, vv. 35, 2006, pp. 583.
- [3] M.A- Ahmed and M.A. El Hiti, Electrical and Dielectric Properties of $\text{Zn}_{0.8}\text{Co}_{0.2}\text{Fe}_2\text{O}_4$, Journal of Physics III, EDP Sciences, vv. 5, 1995, pp. 775-781.
- [4] J.L. Dormann, M. Nogus, Magnetic structures in substituted ferrites, Journal of Phys.: Condensed Matter, vv. 2, 1990, pp. 1223-1237.
- [5] A.S. Teja and P. Y. Koh, Synthesis, properties, and applications of magnetic iron oxide nanoparticles, Progress in Crystal Growth and Characterization of Materials, vv. 55, 2009, pp. 22-45.
- [6] U.T. Lam, R. Mammucari, K. Suzuki, N.R. Foster, Processing of iron oxide nanoparticles by supercritical fluids, Journal of Industrial and Engineering Chemistry Research, vv. 47, 2008, pp. 599.
- [7] G. Dixit, J.P. Singh, R.C. Srivastava, H.M. Agarwal, R.J. Chaudhary, Structural, magnetic and optical studies of nickel ferrite thin films, Advanced Materials Letters, vv. 3, 2012, pp. 21-26.
- [8] W. Yan, Q. Li, H. Zhong, Z. Zhong, Characterization and low-temperature sintering of $\text{Ni}_{0.5}\text{Zn}_{0.5}\text{Fe}_2\text{O}_4$ nano-powders prepared by refluxing method, Powder Technology, vv. 192, 2009, pp. 23-26.
- [9] S.W. Cao, Y.J. Zhu, G.F. Cheng, ZnFe_2O_4 nanoparticles: Microwave-hydrothermal ionic liquid synthesis and Photocatalytic property over phenol, Journal of hazardous materials, vv. 171, 2009, pp. 431-435.
- [10] Y.L. Liu, Z.M. Liu, Y. Yang, Simple synthesis of MgFe_2O_4 nanoparticles as gas sensing materials, Sensors and Actuators B: Chemical, vv. 107, 2005, pp. 600-604.
- [11] V.G. Harris, A. Geiler, Y. Chen, Recent advances in processing and applications of microwave ferrites, Journal of Magnetism and Magnetic Materials, vv. 321, 2009, pp. 2035-2047.
- [12] Y. Qu, H. Yang, N. Yang, The effect of reaction temperature on the particle size, structure and magnetic properties of co-precipitated CoFe_2O_4 nanoparticles, Materials Letters, vv. 60, 2006, pp. 3548-3552.
- [13] N. Kasapoglu, B. Birsoz, A. Baykal, Synthesis and Magnetic Properties of Octahedral ferrite $\text{Ni}_x\text{Co}_{1-x}\text{Fe}_2\text{O}_4$ Nano Crystals, Central European Journal of Chemistry, vv. 5, 2007, pp. 570-580.

- [14] M. Srivastava, A.K. Ojha, S. Chaubey, A. Materny, Synthesis and optical characterization of nanocrystalline NiFe₂O₄ structures, *Journal of Alloys and Compounds*, 481, 2009, 515–519.
- [15] A. Gaffoor, D. Ravinder, Characterization of magnesium substituted Nickel Nano ferrites synthesized By Citrate-Gel Auto Combustion Method, *Journal of Engineering Research and Applications*: 2248-9622, vv. 4, 2014, pp. 60-66.
- [16] D. Varshney, Kavita Verma, Substitutional effect on structural and dielectric properties of Ni_{x-1}A_xFe₂O₄ (A = Mg, Zn) mixed spinel ferrites, *Materials Chemistry and Physics*, vv. 140, 2013, pp. 412-418.
- [17] B.R. Babu, T. Tatarchuk, Elastic properties and antistructural modeling for Nickel-Zinc ferrite-aluminates, *Materials Chemistry and Physics*, vv. 207, 2018, pp. 534-541.
- [18] N. S. Sabri, M. S. Mohd Deni, A. Zakaria, M. Kuma, Effect of Mn doping on structural and optical properties of SnO₂ nanoparticles prepared by mechanochemical processing, *Physics Procedia*, vv. 25, 2012, pp. 233 – 239.
- [19] B. Senthilkumar, R. KalaiSelvan, P. Vinothbabu, I. Perelshtein, A. Gedanken, Structural, magnetic, electrical and electrochemical properties of NiFe₂O₄ synthesized by the molten salt technique, *Materials Chemistry and Physics*, vv. 130, 2011, pp. 285–292.
- [20] A.I. Borhan, A.R. Jordan, M.N. Palamaru, Correlation between structural, magnetic and electrical properties of nanocrystalline Al³⁺ substituted zinc ferrite, *Materials Research Bullatine*, vv. 48, 2013, pp. 2549–2556.
- [21] B.R. Babu, T. Tatarchuk, Elastic properties and antistructural modeling for Nickel-Zinc ferrite-aluminates, *Materials Chemistry and Physics*, vv. 207, 2018, pp. 534-541.
- [22] K.B. Modi, M.C. Chhantbar, P.U. Sharma, H.H. Joshi, Elastic constants determination for Fe³⁺substituted YIG through infra-red spectroscopy and heterogeneous metal mixture rule, *Journal of Materials Science*, vv. 40, 2005, pp. 1247 – 1249.
- [23] S.M. Rathod, A.B. Shinde, Synthesis and characterization of Nanocrystalline NiCuZn Ferrite prepared by Sol-gel auto combustion method, *International Journal of Advancements in Research & Technology*, vv. 1 (6), 2012, pp. 1-4.
- [24] G.P. Joshi, N.S.Saxena, R.Mangal, A.Mishra and T.P.Sharma. Band gap determination of Ni-Zn ferrites. *Journal of Indian Academy of Sciences*, vv. 26(4), 2003, pp. 387-389.